Astron. Astrophys. 221, 250–257 (1989)

ASTRONOMY
AND
ASTROPHYSICS

Near-infrared observations and optical identifications of a few unassociated IRAS sources with dust shells

K.V.K. Iyengar [1], S.K. Ghosh [1], T.N. Rengarajan [1], R.P. Verma [1], S.C. Joshi [2], and R.K. Srivastava [2]

[1] Tata Institute of Fundamental Research, Homi Bhabha Road, Colaba, Bombay 400005, India
[2] Uttar Pradesh State Observatory, Manora Peak, Nainital 263129, India

Received December 8, 1988; accepted March 14, 1989

Summary. We have carried out near infrared observations of twenty six unassociated IRAS sources with dust shells. Twenty of these belong to the group that have IRAS low resolution spectral characteristic (LRSCHAR = 4*n*), classified as stars with carbon rich envelopes. Optical counterparts of 18 of these unassociated sources were identified using Palomar Observatory Sky Survey (POSS) prints.

The programme sources with LRSCHAR = 4*n* as a class appear to have thicker dust shells than Two Micron Sky Survey (TMSS) sources of similar LRSCHAR, as evidenced by their larger *K*–[12] colours (>4.3). They thus represent more evolved sources, with high mass loss rates and are perhaps variables with periods >400 days. Their [12]–[25] and [25]–[60] colours are typical of black bodies with temperatures ranging from 400 to 1200 K. The average *K*–[12] and [12]–[25] colours decrease with increasing SiC index, suggesting that the fractional abundance of SiC grains decreases with increasing mass loss rate.

Key words: infrared radiation – stars: carbon – circumstellar – mass loss

1. Introduction

The Infrared Astronomical Satellite Point Source Catalogue (IRAS PSC, 1985) contains about 250000 entries of which 66% are stellar objects. Approximately 81000 of these stars have circumstellar shells (Habing, 1987). A large number of entries in IRAS PSC is not associated with objects in any of the available catalogues (with which associations have been sought in the IRAS PSC) either because they are extremely faint (thereby escaping detection in the previous surveys), or are located in regions of the sky which were not part of the search areas of previous surveys.

In this paper we report on the near infrared detection and optical identification (from POSS prints) of 26 unassociated sources with dust shells, and discuss the results on the basis of infrared colour-colour plots.

2. Observations

2.1. Near-infrared photometry

The observations were undertaken to study a sample of unassociated IRAS selected carbon stars and to compare their infrared colours with those of identified carbon stars. We selected sources satisfying the following criteria: i) No association listed in IRAS PSC, ii) $1.2 < F(12)/F(25) < 3$ where $F(12)$ and $F(25)$ are the 12 μm and 25 μm flux densities listed in IRAS PSC, and iii) characterised by LRSCHAR = 4*n* in the catalogue of Low Resolution Spectra (IRAS Explanatory Supplement, Beichman et al., 1985). Condition (ii) was used to select sources with a moderate quantity of circumstellar material. We further restricted our observations to $3^h < \alpha < 9^h$ and $18^h < \alpha < 20^h$ and $\delta > -15°$, based on the availability of sources during our observing season. Of the 57 sources satisfying the above criteria, we were able to observe 20 sources, in the limited time available to us. The LRS spectra of these sources were also visually inspected by us. We also observed 6 sources satisfying criteria (i) and (ii) but not appearing in the Low Resolution Spectra (LRS) Catalog.

The observations were carried out using an InSb photometer at the *f*/13 Cassegrain focus of the 102 cm telescope at either the Uttar Pradesh State Observatory (UPSO), Nainital, India (lat. = 29°.36 N, long. = 79°.46 E) or at the Vainu Bappu Observatory (VBO), Kavalur, (lat. = 12°.58 N, long. = 78°.83 E). The beam was chopped (using a vibrating tertiary mirror close to the focal plane) at a frequency of 20 Hz. A field of view of 30″ was used and the chopper throw was set at ~40″. The mean differences and rms errors in Right Ascension (R.A.) and Declination (Dec.) of the near infrared positions of the observed sources with respect to their IRAS positions were +2 and 17″, and +4 and 14″, respectively. These errors were mostly due to problems in the offset system of the telescopes. In Table 1, we present the journal of observations.

2.2. Optical identifications

All the programme objects (except one) were searched for optical counterparts on the Palomar Observatory Sky Survey (POSS) prints. The search procedure was similar to that of Ghosh et al. (1984). The R.A. and Dec. and the diameters of the images of optical objects (if any) on both the O and E prints within the IRAS error ellipse were then determined. Whenever there was only one optical object within or on the boundary of the error ellipse in the E print and the chance probability of finding an object greater than or equal to this diameter was <10%, it was identified as the optical counterpart. When multiple sources were present, the brightest with the highest $P-R$ colour was identified as the optical counterpart if it was the only image with the chance probability of finding it <10%. In other cases no identifications were made. Whenever no object was present in the error ellipse,

Send offprint requests to: K.V.K. Iyengar

Table 1. Journal of observations

Date (1)	Telescope (2)	Bands (3)	Calibration stars (4)	IRAS sources observed (5)
20/21-01-1987	UPSO	*K*	λ Tau, ε Eri	05581+2232
			10 Tau, α Leo	06039+0956
			BS 4030	
			BS 4550	
21/22-01-1987	UPSO	*K*	α Per, ε Eri	05013+1128
			α Leo	05588+2149
			BS 1790	06104+1345
			BS 3176	06378−0527
			BS 4550	06564+0342
24/25-01-1987	UPSO	*K*	λ Tau, 33 Psc	03277+5120
			ξ Ceti, λ Aur	03385+5927
			ν UMa, η Vir	04165+1420
			BS 3176	04340+4623
				05316+1757
				06348+3114
				06487+0551
				07170+0721
				08427+0338
10/11-04-1987	UPSO	*JHK*	α CMi, α Leo	06378−0527
			ν Her	06564+0342
			BS 4550	08129−1236
				17581−1744
22/23-04-1988	VBO	*JHK*	α CMi, ν Her	06378−0527
			BS 2318	08129−1236
			BS 4550	08427+0338
			BS 6136	17581−1744
			BS 7615	18424+0346
			SJ 9523	18430−0032
				18520−0221
				19108+1155
				19289+1931
				19346+1209
				19419+3222
				19523+2414

only limits were assigned to their magnitudes. The *P* and *R* magnitudes of the identified objects were estimated (to better than 1 mag) from their diameters on the O and E prints using the relation given by King and Raff (1977). The optical fields of these sources as seen on POSS prints are shown in Fig. 1a–d and the results are given in Table 2. Out of a total of 25 sources searched for, 18 have optical counterparts, 4 have no optical counterparts ($P > 21$ mag and $R > 20$ mag) and three are in confused regions. From an examination of the infrared magnitudes and colours of the 4 objects with no optical counterparts, no unusual characteristic is observed. However, one source 19523+2414 is at the edge of an isolated dark cloud. The mean differences and the rms deviations between the IRAS and optical positions are +2, and 11″ in R.A. and +1, and 6″ in Dec. respectively.

3. Results

The photometric data presented in Table 2, in columns 1–10 are: the IRAS name of the source, IRAS position (1950), IRAS-optical positional differences, the *P* and *R* magnitudes, the *K*, *H*, and *J* magnitudes from the present study, the [12], [25], and [60] magnitudes obtained from IRAS data after colour correction (see IRAS Explanatory Supplement, Beichman et al., 1985), the LRSCHAR type and the IRAS Variability index. Although all the programme objects were detected in the *K* band, *J* and *H* measurements could be carried out for only 12 of them.

4. Discussion

4.1. [*H*−*K*] *versus* [*J*−*H*]

We show in Fig. 2 the [*H*−*K*] versus [*J*−*K*] colours for the programme sources of LRSCHAR = 4*n* for which these data are available along with the average value for the Two Micron Sky Survey (TMSS; Neugebauer and Leighton, 1969) stars obtained from the data presented by Claussen et al. (1987) in their Table 2. It is seen that the programme sources have higher values of [*J*−*H*] and [*H*−*K*] and are highly reddened as compared to TMSS stars, as expected from our selection criteria.

4.2. [12]–[25] *versus* *K*–[12]

Presented in Fig. 3a is a plot of [12]–[25] versus *K*–[12] of the 20 programme sources with LRSCHAR = 4*n* along with stars from the TMSS with LRSCHAR = 4*n*. While the *K* magnitudes for the programme sources are from the present work, those for the TMSS sources are from Neugebauer and Leighton (1969).

Most of the programme sources are variable as indicated by the IRAS variability index listed in Table 2. 65% of 20 sources with LRSCHAR = 4*n* have a variability index >90, indicating a >90% probability of variability between the different hours-confirming scans. On the other hand, out of 6 sources not having LRS spectra and observed by us in the near-IR, only one has a variability index >90. Five of the 26 sources, were reobserved by us at times separated by a few months. All of these were found to have a variability of >0.2 mag in the *K* band. The programme sources with LRSCHAR = 4*n* have *K*−[12] > 4 from which one can infer periodicity of $\gtrsim$400 days (Jura, 1986).

Rowan-Robinson and Harris (1983) and Rowan-Robinson et al. (1986) have analysed the near infrared and IRAS spectra of carbon stars. They find a reasonable fit on the basis of a model with the following parameters: stellar temperature of 2000 K, amorphous carbon grains with a density distribution $n(r) \propto r^{-2}$, a dust shell characterised by an inner radius of temperature 1000 K and a parameter τ_{uv} representing the radial optical depth for the absorption of optical photons. They find that as τ_{uv} increases, both the *K*–[12] and [12]–[25] colours increase. The distribution of our sources in the [12]–[25] versus *K*–[12] plot is as per model calculations with τ_{uv} varying from 20 to 0.5. The twenty 4*n* sources observed by us belong to group III carbon stars with high mass loss as defined by Willems (1987). Most of the TMSS sources with LRS spectra occupy lower *K*–[12] portion of the plot, consistent with the brightness limits set for both *K* and [12] magnitudes. Their colours show that they mostly belong to group II sources (Willems, 1987) having lower dust optical depth where the contribution of the stellar photosphere is significant.

In Fig. 3b, we show a plot of average values of [12]–[25] versus *K*–[12] as a function of *n*, the SiC index. It may be noted that the SiC index represents 10 times the logarithmic ratio of the observed flux density at 11.4 μm, the peak of the SiC feature, to that at the

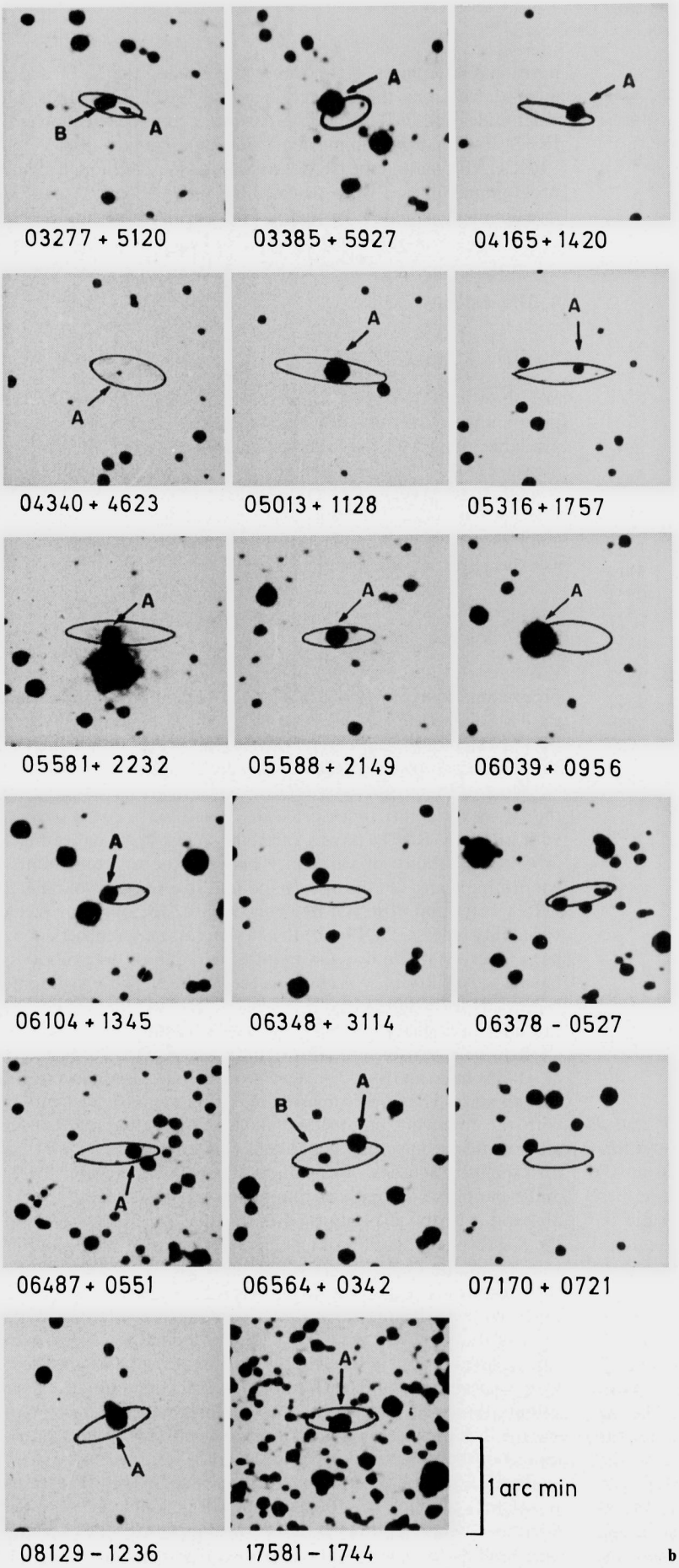

Fig. 1a and b. Fields of programme sources as shown on POSS E prints. The ellipses shown are centered (to better than 5″) on the IRAS positions of the sources and have axial dimensions and position angles as listed in IRAS PSC. Whenever more than one optical object is found in the error ellipse, the one labelled *A* is considered to be the most probable optical counterpart of the source as judged from its proximity to the IRAS position and its [*P*–*R*] colour

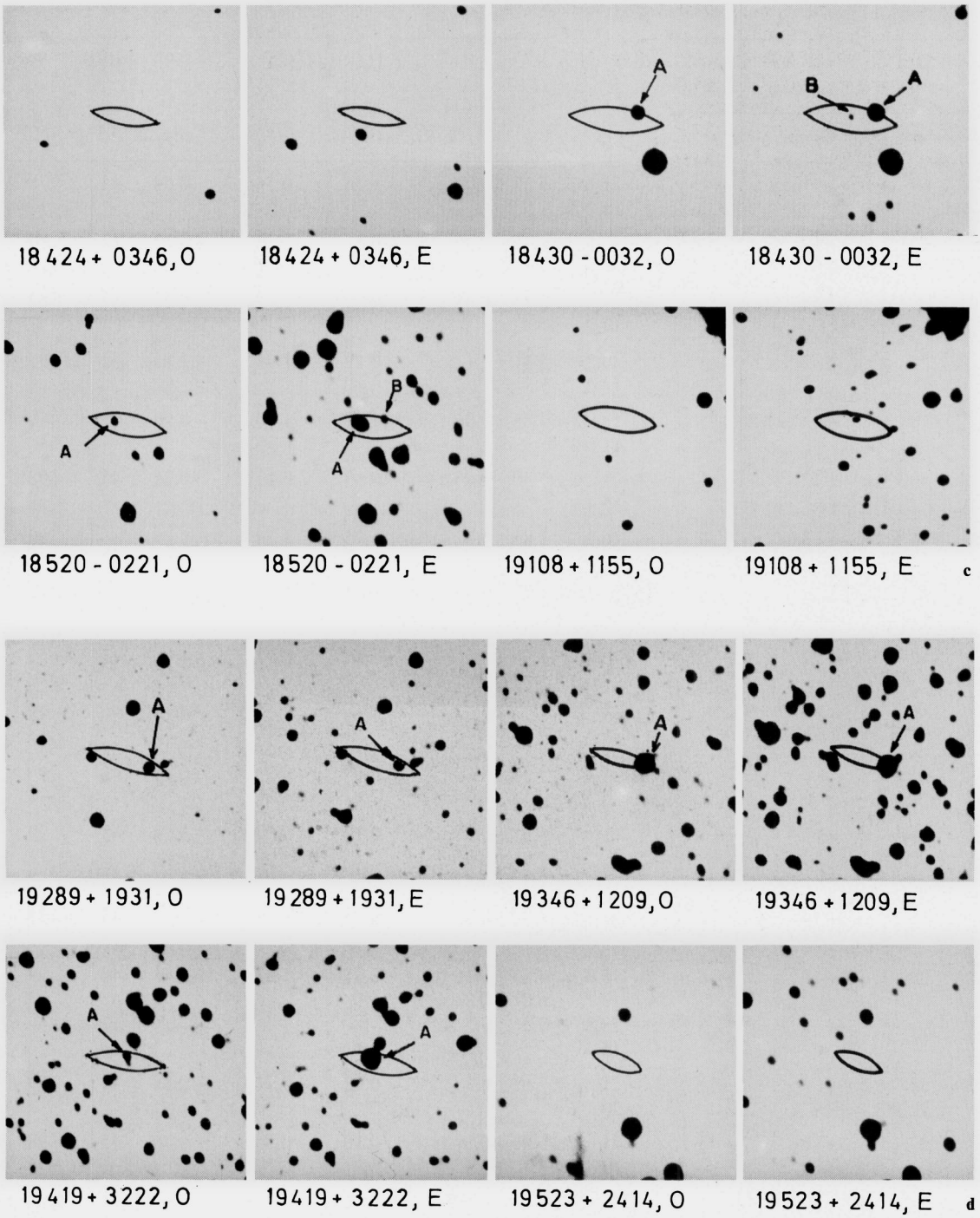

Fig. 1c and d. Same as in Fig. 1a and b with fields as seen on both O and E POSS prints

continuum interpolated between 9.8 and 13.3 μm. This index is a measure of the abundance of SiC grains relative to the grains responsible for the continuum emission. Van der Veen and Habing (1988) have shown that for the complete sample of 4 *n* sources, the [12]–[25] colour decreases as *n* increases. Such a behaviour is seen in our plot also. In addition it is seen that, the average *K*–[12] colour also decreases with increasing *n*. From the models of Rowan-Robinson and Harris (1983), we can infer that increasing colours indicate larger τ_{uv}, i.e., higher mass loss rate for the stars. The variation of colour with SiC index can be interpreted as decreasing fractional abundance of SiC grains as the total dust column density (mass loss rate) increases. This is in agreement with the finding of Skinner and Whitmore (1988) who find that the ratio of the luminosity in SiC feature to $\dot{M}$ (a measure of the total dust column) is $\propto \dot{M}^{-0.33}$, where $\dot{M}$ is the rate of mass loss.

In Fig. 3b, we have also plotted the average colours as a function of *n* for all TMSS objects having [12]–[25] > 0.35, the same limit as for our sample. It is seen that the same trend of

Table 2. Near infrared observations of IRAS unassociated sources

IRAS name	RA (1950) (s)	Dec. (″)	IRAS−Optical $\Delta\alpha$(″)	IRAS−Optical $\Delta\delta$(″)	P R	K H J	[12]	[25]	[60]	LRS	Var.
(1)	(2)		(3)		(4)	(5)	(6)	(7)	(8)	(9)	(10)
03277+5120	44.5	09	− 1	− 1	>21 (a) 14.2	5.37±0.06	1.06	0.54	0.34	44	78
03385+5927	34.1	30	−12	− 6	12.6 11.0	6.45±0.06	−0.61	−1.55	−1.42	42	99
04165+1420	30.8	03	+14	+22	>21 14.2	5.35±0.05	0.99	0.63	0.53	47	62
04340+4623	01.2	27	− 2	+ 3	20.3 18.0	7.1 ±0.1	−0.19	−1.44	−1.85	42	95
05013+1128	18.2	40	+ 3	+ 1	18.9 11.0	4.56±0.06	1.52	1.10	0.90	–	–
05316+1757	40.1	56	+12	− 1	>21 15.4	5.50±0.05	0.63	0.17	−0.21	45	98
05581+2232	10.4	55	− 3	0	16.5 14.2	3.85±0.02	1.75	1.34	0.89	–	80
05588+2149	51.5	06	− 3	− 2	17.4 13.4	3.51±0.03	1.62	1.09	>1.18	–	1
06039+0956	57.7	52	−22	+ 5	10.9 10.0	5.78±0.06	1.46	0.98	1.00	–	59
06104+1345	27.2	57	− 9	− 1	>21 14.2	5.24±0.04	1.68	1.22	0.13	–	98
06348+3114	50.9	23			>21 >20	5.50±0.05	0.45	−0.33	−0.63	42	96
06378−0527	51.3	11			(b)	5.51±0.68 (c) 7.2 ±0.2 9.7 ±0.5	0.13	−0.69	−1.54	43	99
06487+0551	44.8	10	+14	− 2	>21 14.2	4.70±0.05	−0.66	−1.28	−1.54	43	31
06564+0342	27.1	08	+10	− 8	15.0 13.1	4.68±0.10 (c) 6.8 ±0.2	−0.25	−1.03	−1.41	44	99
			− 9	+ 3	18.8 15.4	9.5 ±0.5					
07170+0721	03.9	32			>21 >20	7.6 ±0.1	0.02	−0.74	−0.88	44	99
08129−1236	58.0	07	+ 6	− 3	>21 13.4	5.96±0.31 (c) 8.1 ±0.5 >9.0	0.16	−0.54	−0.70	45	98
08427+0338	45.6	10			(d)	6.04±0.23 (c) 7.6 ±0.2 >7.7	1.90	1.50	1.20	–	63
17581−1744	11.4	20	+ 3	+ 3	14.8 12.2	4.34±0.09 (c) 6.40±0.06 8.6 ±0.6	−0.54	−1.21	−1.53	44	99
18424+0346	29.2	25			>21 >20	3.93±0.02 5.25±0.05 7.1 ±0.4	−0.43	−1.18	−1.60	44	97
18430−0032	02.7	26	+17	+ 4	15.3 13.8	5.18±0.04 6.40±0.05 8.4 ±0.3	0.79	0.13	>−3.55	45	70

Table 2 (continued)

IRAS name	RA (1950) (s)	Dec. (″)	IRAS−Optical $\Delta\alpha$(″)	$\Delta\delta$(″)	P R	K H J	[12]	[25]	[60]	LRS	Var.
(1)	(2)		(3)		(4)	(5)	(6)	(7)	(8)	(9)	(10)
18520−0221	03.8	49	+ 5	− 2	18.3 14.4	5.73±0.02 7.1 ±0.1 9.5 ±0.5	0.85	0.15	> −0.81	46	26
19108+1155	53.1	02			(b)	5.98±0.02 7.7 ±0.1 >9.7	0.20	−0.30	−0.87	44	88
19289+1931	56.5	49			(b)	7.4 ±0.1 > 9.5 >10.3	−0.29	−0.88	−0.26	42	99
19346+1209	39.1	52	+17	+ 6	13.7 13.5	8.4 ±0.3 > 8.8 > 8.8	0.18	−0.75	−1.15	43	99
19419+3222	56.1	11	− 2	− 2	17.6 12.9	5.41±0.03 6.60±0.06 8.6 ±0.3	0.31	−0.23	−0.10	44	98
19523+2414	21.9	25			>21 >20	6.38±0.6 8.7 ±0.4	0.55	−0.26	−0.47	43	56

Notes to Table 2: (a) There are two optical objects viz., A and B in the error ellipse. A has P and R of >21 and 14.2, whereas B has P and R of 17.3 and 16.3. A is identified as the optical counterpart. (b) Confusing. (c) Errors indicated are not photometric; they indicate phase dependent variations in the magnitude due to variability. (d) No search could be made for the optical counterpart as the particular POSS print was not available to us.

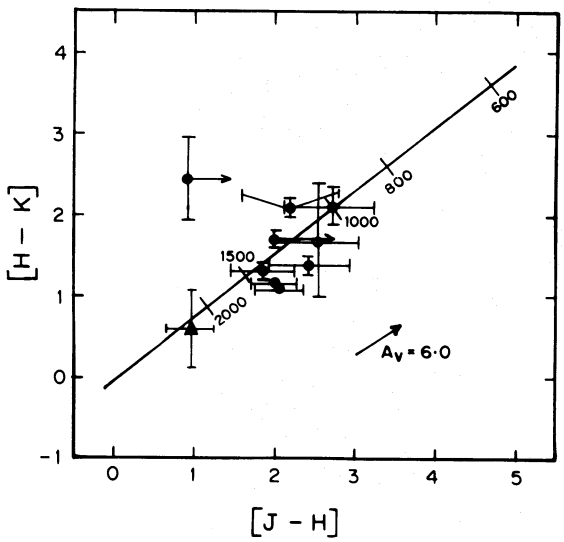

Fig. 2. Colour-colour diagram of $[J-H]$ versus $[H-K]$. The symbol ● refers to data points of sources with LRSCHAR = 4 n detected in the present work. The flags on the data points indicate the photometric errors on the colours. The symbol ▲ refers to the mean value and the flags on it to the rms of the $[J-H]$ versus $[H-K]$ colours of the TMSS sources (classified as carbon stars) for which photometric data are listed in Table 2 of Claussen et al. (1987). The vector in the lower right hand bottom of the figure shows the reddening corresponding to $A_v = 6.0$ mag (Frogel and Whitford, 1987)

decreasing [12]–[25] as n increases is seen. However, the K–[12] colour does not decrease monotonically. This is understandable since the K magnitudes for these sources with optically thinner dust shells are closer to the photospheric values.

4.3. [25]–[60] *versus* [12]–[25]

In a plot of [25]–[60] versus [12]–[25], IRAS selected carbon stars are mostly seen to lie close to the black body line with temperatures ranging from 500–1200 K (Willems, 1987; Nguyen-Q-Rieu et al., 1987). In Fig. 4 we give such a plot for our programme sources superposed in Fig. 5 of Nguyen-Q-Rieu et al. (1987) which incorporates their data points for unassociated IRAS 4 n sources with CO, HCN detections along with CO-IR stars from Knapp and Morris (1985), Zuckerman et al. (1986), and Zuckerman and Dyck (1986a, 1986b). Most of our sources are also close to the black body line. Three sources (03385+5927, 19289+1931, and 19419+3222) have rather low [25]–[60] colours indicating scarcity of cool dust. Of these, two are also optically bright, as indicated by their P and R magnitudes. The six sources with no LRS observations (not shown in the figure), occupy a region intermediate to that of the bulk of the TMSS and our 4 n sources in the [12]–[25] versus K–[12] plots. In the [25]–[60] versus [12]–[25] plots also all except 06104+1345 lie close to the black body line.

5. Conclusions

Near-infrared observations of 26 unassociated IRAS sources with $1.2 < \{F(12)/F(25)\} < 3$ of which 20 have LRSCHAR = 4 n show

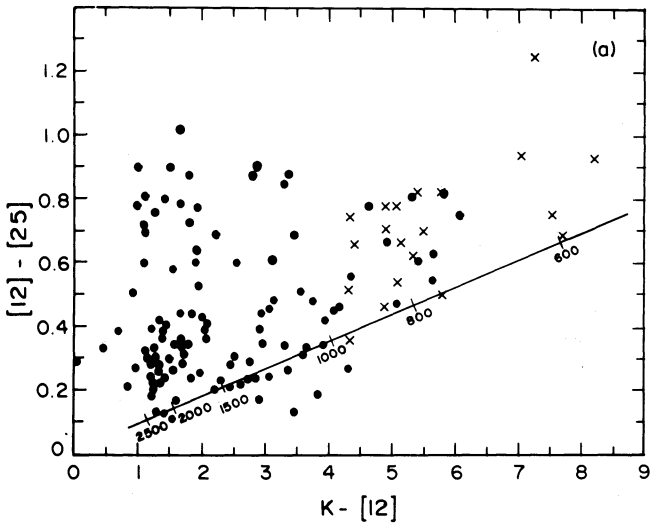

Fig. 3a. Colour-colour diagram of $K-[12]$ versus [12]–[25]. The ×'s refer to data points of programme sources of LRSCHAR = 4*n*. The ● are the data points of TMSS sources with LRSCHAR = 4*n* as determined from IRAS LRS data. The solid line is the locus for black body emission with temperatures indicated by the tick marks against them

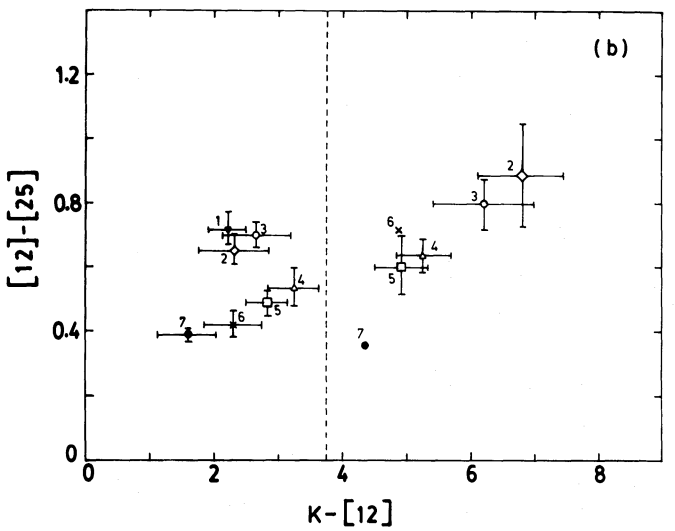

Fig. 3b. Colour-colour diagram of $K-[12]$ versus [12]–[25] of programme sources and TMSS stars of LRSCHAR = 4*n*. The symbols ▼, ◇, ○, △, □, ×, and ● show the mean colours with their rms for sources of LRSCHAR 41, 42, 43, 44, 45, 46, and 47 respectively. The dashed line is drawn to distinguish the TMSS sources to its left from the programme sources to its right. No error bars are shown on the data points ×, ● of programme sources as these are based on the datum of only one source of each type

that they have $K-[12]$ colours higher than those of TMSS stars of same LRSCHAR. They appear to be stars with high mass loss rates. Based on the models of Rowan-Robinson and Harris (1983), the distribution in the [12]–[25] versus $K-[12]$ plot indicates a range of 20 to 0.5 for τ_{uv}. The decrease of their [12]–[25] and $K-[12]$ colours with increasing SiC index appears to be due to the decreasing fractional abundance of SiC grains as the total column density (mass loss rate) increases.

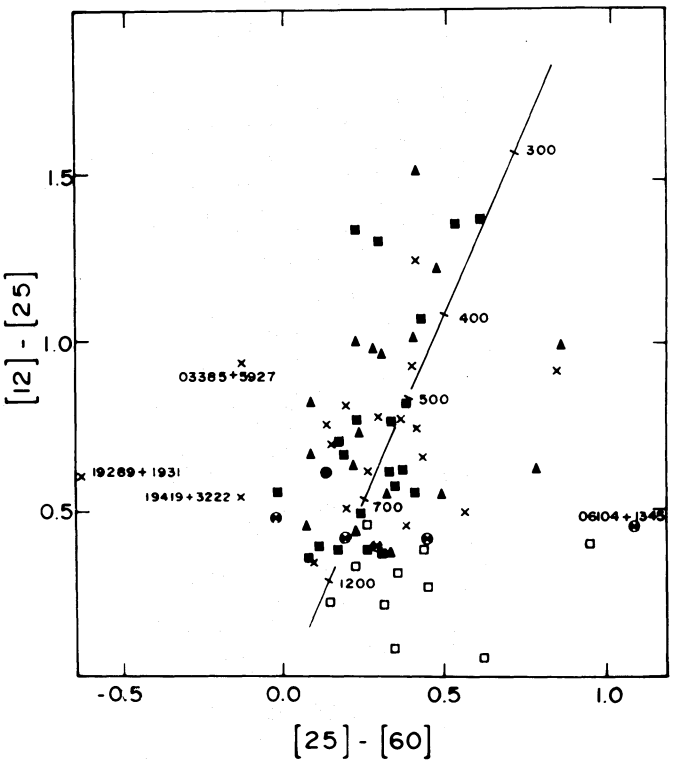

Fig. 4. Colour-colour diagram of [25]–[60] versus [12]–[25] of carbon stars. The symbols ▲, ■, and □ are data points of carbon stars as presented in Fig. 3 of Nguyen-Q-Rieu et al. (1987). The ▲ refers to data points of CO-IR IRAS stars detected by them; the ■, and □ refer to unidentified objects and optically visible CO-IR stars reported in the literature (see Nguyen-Q-Rieu et al., 1987). The ×'s and ⊗ are the data points of programme sources from this work of LRSCHAR = 4*n* (carbon stars) and the ones that do not have LRS spectra, respectively. The solid line is the locus for black body emission with temperatures indicated by the tick marks against them

Acknowledgements. We thank the Directors of the Uttar Pradesh State Observatory, Nainital, U.P., and the Vainu Bappu Observatory of the Indian Institute of Astrophysics, Bangalore, for kindly allotting us telescope time and the staff of these observatories for support during the observations. We thank Professor S.P. Tarafdar for useful discussions. We also thank Mr. M.V. Naik for his help with the electronic instruments and Mr. H.T. Saraiya in the data analysis.

References

Claussen, M.J., Kleinmann, S.G., Joyce, R.R., Jura, M.: 1987, *Astrophys. J. Suppl.* **65**, 385

Frogel, J.A., Whitford, A.E.: 1987, *Astrophys. J.* **320**, 199

Ghosh, S.K., Iyengar, K.V.K., Rengarajan, T.N., Tandon, S.N., Verma, R.P., Daniel, R.R.: 1984, *Monthly Notices Roy. Astron. Soc.* **206**, 611

Habing, H.J.: 1987, *The Galaxy*, eds. G. Gilmore, B. Carswell, Reidel, Dordrecht, p. 173

IRAS Explanatory Supplement: 1985, eds. C.A. Beichman, G. Neugebauer, H.J. Habing, P.E. Clegg, T.J. Chester, U.S. Government Printing Office, Washington, DC

IRAS Point Source Catalog: 1985, Joint Science Working Group, U.S. Government Printing Office, Washington, DC

King, I.R., Raff, M.I.: 1977, *Publ. Astron. Soc. Pac.* **89**, 120
Jura, M.: 1986, *Astrophys. J.* **303**, 327
Knapp, G.R., Morris, M.: 1985, *Astrophys. J.* **292**, 640
Neugebauer, G., Leighton, R.B.: 1969, *The Micron Sky Survey*, NASA, SP-3047
Nguyen-Q-Rieu, Epchtein, N., Truong-Bach, Cohen, M.: 1987, *Astron. Astrophys.* **180**, 117
Rowan-Robinson, M., Harris, S.: 1983, *Monthly Notices Roy. Astron. Soc.* **202**, 797
Rowan-Robinson, M., Lock, T.D., Walker, D.W., Harris, S.: 1986, *Monthly Notices Roy. Astron. Soc.* **222**, 273
Skinner, C.J., Whitmore, B.: 1988, *Monthly Notices Roy. Astron. Soc.* **234**, 79P
Van der Veen, W.E.C.J., Habing, H.J.: 1988, *Astron. Astrophys.* **194**, 125
Willems, F.J.: 1987, Ph. D. Thesis, *Infrared Studies of Asymptotic Giant Branch Stars*, University of Amsterdam
Zuckerman, B., Dyck, H.M., Claussen, M.J.: 1986, *Astrophys. J.* **304**, 401
Zuckerman, B., Dyck, H.M.: 1986a, *Astrophys. J.* **304**, 394
Zuckerman, B., Dyck, H.M.: 1986b, *Astrophys. J.* **311**, 345